Uncertainty in cell confluency measurements

G. Sassi
Dipartimento di Scienza dei Materiali e Ingegneria Chimica
Politecnico di Torino
Torino, Italy

S. Pavarelli, C. Divieto, M.P. Sassi
Istituto Nazionale di Ricerca Metrologica INRIM
Torino, Italy
m.sassi@inrim.it

***Abstract*—Pharmaceutical industries have declared their need of metrology in the cellular field, to improve new drugs developing time and costs by high-content screening technologies. Cell viability and proliferation tests largely use confluency of cells on a bi-dimensional (2D) surface as a biological measurand. The confluency is measured from images of 2D surface acquired via microscopy techniques. The plethora of algorithms already in use aims at recognizing objects from images and identifies a threshold to distinguish objects from the background. The reference method is the visual assessment from an operator and any objective uncertainty estimation is not yet available. A method to estimate the image analysis contribution to confluency uncertainty is here proposed. A maximum and a minimum threshold are identified from a visual assessment of the free edge of the cells. An application to a fluorescence microscopy image of 2D of PT-45 cell cultures is reported. Results shows that the method can be a promising solution to associate an uncertainty to cell confluency measurements to enhance reliability and efficiency of high-content screening technologies.**

Keywords—Cell Confluency; Image analysis; Measurement Uncertainty; High Throughput Screening; Drug development.

I. INTRODUCTION

High-content screening (HCS) technologies strongly support cell-based imaging assays, e.g., such as automated immunostaining, automated image acquisition and automated image analysis [1]. Assays are constantly under development to improve, make faster and simplify the data analysis. As clearly stated by Xia and Wong [2], HCS is considered a "cellular image-based high-throughput screening" (HTS): the combination of HTS and microscopy led to the HCS technology which allows automated acquisition and analysis of data coming from cell behaviors which are highly informative about what it is happening in the cell culture [2, 1, 3]. In a HCS, each single cell is specifically and fluorescently stained to be analyzed at a sub-cellular level (micrometer resolution) [4].

HCS are widely adopted in drug development and discovery, toxicology analysis on cell models, research on infectious diseases and in cell biology basic research. In addition, it is a promising methodology for personalized medicine and stem cells research [4, 2, 3]. HCS allow quick evaluation of the effects of thousands of molecules on cells and provide starting points for drug design and for understanding the interaction or role of particular biochemical processes [5]. Cell morphology, cell proliferation, cell migration are only some of the aspects being studied in phenotypic screening for cellular pathways, cell functions and biological mechanism by adopting the cell image analysis of HCS technology [2, 6, 7].

Automated cell image analysis is employed for several research purposes: to measure single cell and colony shape, density, size, location, co-localization, texture, intensity and several other features in cell culture [8, 9]; to measure the cell morphometry in bone growth *in vivo* studies [10]; to analyze cell migration in living cells in culture [11]; to analyze the biomarker distribution in tumor cells [12]; to detect the presence of tumor cells in tissue samples [13]: to measure HIV particles neutralization performed by neutralizing antibodies [14].

In the cell image analysis, confluency of cells on a bi-dimensional (2D) surface, i.e., the fraction of surface area occupied by cells, is a measurand easily defined and realized that account for several complex features of cell model in culture, such as biological effect of a molecule under examination. It is know that variability in cell confluency can affect the HTS and HCS analysis [15]. Reproducible confluency may assure a reproducible generic activity of cells as a reproducible reference initial condition for assays.

Cell confluency is measured in cell cultures to monitor the cell growth during a treatment and to modulate the subculture in 2D and 3D cell culture [16, 17, 18, 19], to perform toxicity tests with chemical or drug treatment at a certain cell confluency % [20, 21], to measure tumor cell proliferation *in vitro* [22], in drug development to find cytoplasm abnormalities discriminating between areas with cells (occupied by cells) and areas no cells (background) [3]. Cell confluency has been found to affect the expression of cell surface markers in studies on murine stem cells [23], to have effect on the cell stiffness [24], intracellular forces [25] and on the cell cycle [26], to have a critical impact in gene expression in adipose stromal cells [27]. Cell confluency is the first visual assessment in drug discovery and toxicology screening, where HTS and HCS are applied: cells seeded at an initial number, should not be over or sub-confluence in order not to lose genetic or physiological characteristics to analyzed [28].

The confluency measurement is obtained through analysis of images acquired via microscopy techniques [3, 9]. HCS integrates fluorescence microscopy and algorithms for image analysis to automate cell analysis [6]. This allows to obtain confluency measurement as the first and easiest parameter from

978-1-4799-6477-2/15/$31.00 ©2015 IEEE

where collect information on the cell model system behavior over time. The automated image analysis aims at recognizing objects and typically identifies a single threshold value to distinguish objects (foreground) from the background, an extremely wide range of algorithms is available [29, 30].

To date, the operator's experience in visual assessment of images remains the most reliable reference for confluency quantification in the totality of developed algorithms and an objective estimation of measurement uncertainty has not yet been taken into account. An uncertainty evaluation of the cell confluency measurement can give a strong support to the need of having fast results with low number of repetitions. Uncertainty sources for confluency measurement come from both image acquisition and image analysis depending on their methods and methodologies.

The pharmaceutical industries have declared their need of metrology in the cell-based assays field, in order to improve reliability and comparability of results, reduce the number of the tests, narrow the time from discovery to the marketing of new drugs and limit costs [31]. HCS are expected to develop more and more in the next future thanks to improved algorithm, and detection methods [6]. An effective way to improve algorithms is the knowledge about their robustness as accuracy and reproducibility of results. Confluency measurement uncertainty is here considered as a contribution to improve HCS technologies efficiency. The stakeholders and end-users of the confluency measurement have not officially declared a target uncertainty and the typical step of a traditional visual assessment (5-10%) can be considered as a reference value for actual uncertainty.

This work proposes a method for the estimation of the contribution of the image analysis to the uncertainty of the confluency measurement. The method identify an uncertain area by the visual assessment of the free edge of cells and the quantification of a maximum threshold value and a minimum threshold value. Its application to images, acquired in fluorescence microscopy, of 2D cell cultures of PT-45 cells (pancreatic carcinoma cell line) is reported. It can be a promising solution to associate an uncertainty to cell confluency measurements to enhance the high-content screening technologies reliability and efficiency.

II. Materials and Methods

A. 2D cell cultures

Human pancreatic carcinoma cell line PT-45 from primary tumor (provided by Institute for Cancer Research, Candiolo, Italy) are ZsGreen1 positive showing an emitted fluorescence at 505 nm when excited at 493nm from the whole cytoplasm. Cells were grown in Dulbecco's Modified Eagle's Medium (DMEM) supplemented with 10% Fetal Bovine Serum (FBS), 2 mM glutamine, 0.0625 mg/ml of penicillin, and 0.1 mg/ml streptomycin (Sigma-Aldrich). Cells were maintained at 37°C in a humidified atmosphere with 5% CO_2. Cells were seeded in 3 Petri dishes at the cell density of 5, 10 and 20×10^3 cells/cm^2 to obtain a low (L) medium (M) and high (H) cell confluency (fig. 1). Cells were maintained at 37°C in a humidified atmosphere with 5% CO_2 for 24 hours before imaging.

B. Cell image acquisition

An optical microscope (Zeiss Axio Observer.Z1) with a black and white, high resolution digital CCD camera (Olympus XM10, 1.4 megapixel, 14 bit) was used to image the cells. Images were recorded under uniform illumination in a bright field, using objectives ×10, to produce images at ×100 apparent magnification. Mercury vapor lamp was used as the illumination source. Digital images were collected with the Axio Observer.Z1 Software. Images were captured in high-quality format, corresponding to an image of 16 bit with an exposure time ranging from 200 to 500 milliseconds. Each image was acquired at five different focal planes with z defined by the operator using the software of Axio Observer.Z1. The five focal planes were chosen for each image as follow: the right focal plane (the best focus seen by the operator's eye), "0", two at "0 ± 5 µm" and other two at "0 ± 10 µm". For all images, intensity was scaled on 16 bit integer between max and min fluorescence intensity to limit images variability. On each dish, three different zones were sampled.

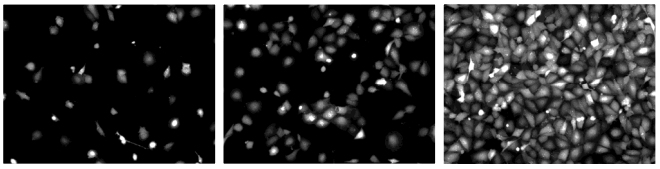

Fig. 1. Fluorescence microscopy images PT-45 living cells at low (L) medium (M) and high (H) cell density (Samples 2) at best focus.

C. Confluency and uncertainty calculation

The confluency was defined as the fraction of pixels in the image foreground, i.e., the ratio between the number of pixel attributed to foreground and the number of pixel in the whole image.

1) Visual Assessment

A visual assessment was performed on each image to identify the free edges between cells and background. The intensity of the pixel and its belonging or not to a form due to a cell were considered to discriminate between background and foreground. Contrast was modified to enhance edge visibility. A binary map from each image identifies foreground (white) and background (black) pixel sets. Three independent visual assessments were repeated three times.

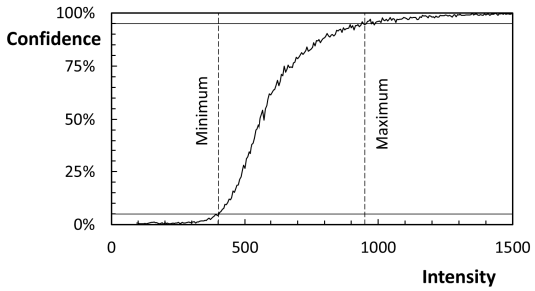

Fig. 2. Confidence to not have background pixels at the fluorescence intensity level for sample H1.

2) Threshold value

A minimum intensity and a maximum intensity were identified as upper and lower threshold value limit respectively.

Below the lower threshold, the confidence to not have foreground pixels is greater than 95% pixels. Over the upper threshold considers the confidence to not have background pixels is greater than 95% pixels (ref. Fig. 2). The fraction of foreground pixel at each fluorescence intensity level was considered as an estimation of the confidence to not have background pixels at the intensity level. Intersections between binary map sets and iso-intensity sets identify the fraction in each set at the intensity level. A minimum number of pixels at each intensity level was ensured by the wideness of intensity assigned to the level to have a meaningful evaluation of confidence.

3) Uncertainty of confluency

The edge of contour that separates foreground (cells) from the background was considered as a subset of boundary, i.e., a subset of the set of pixels with intensity between upper and lower threshold value. The pixels belonging to the boundary were considered of uncertain assignment when a single threshold is used to discriminate foreground from background. The pixel with scaled intensity over the upper threshold were considered to belong to the foreground. The pixel with scaled intensity below the lower threshold were considered to belong to the background. The uncertainty was calculated as type B, as indicated in [32], assuming a normal distribution of the pixel belonging to the edge contour and a 95% membership to the edge boundary.

4) Confluency.

The confluency fraction definition was realized in different ways as calculation method for the most probable free edge:

1. Visual Assessment, the fraction of foreground pixels in the binary map of visual assessment;
2. Mean Area, the mean between the fraction of foreground pixels in the image and the complement to one of the fraction of background pixels in the image (double threshold);
3. Mean Threshold, the fraction of pixels with intensity larger than the mean intensity between upper and lower threshold value (single threshold);
4. Median Threshold, the fraction of pixels with intensity larger than the intensity at 50% confidence (single threshold).

Reproducibility for each calculation method was calculated as type B, as indicated in [32], assuming a uniform distribution on the range. The uncertainty due to calculation method was calculated for each image as type B, as indicated in [32], assuming a uniform distribution on the range. The variability of confluency and its uncertainty due to focus plane variation was calculated as type B, as indicated in [32], assuming a uniform distribution on the range. Significant index values of calculation method and variability contribution to uncertainty were calculated for each image as a ratio between squared contributions [33].

III. RESULTS:

The method has been applied to images, acquired in fluorescence microscopy, of 2D cell cultures of PT-45 living cells (pancreatic carcinoma cell line). The intensity was scaled on minimum to maximum fluorescence intensity range at 16 bit integers to harmonize image acquisition. Background average level in the flat zones was the same for all the scaled images.

A. Threshold levels

For each image, a visual assessment to identify the surface area covered by cells was performed and resumed in a binary map. As a first result, the free edges between cells and background are under the 3% of maximum intensity. Scaled fluorescence intensity levels at 5%, 50% and 95% confidence are reported in Table I for each confluency level as a mean of all samples. Fluorescence threshold values are different even if the background has similar intensity level in the flat zones. Mean lower threshold and median intensity have similar values at all confluency level while upper threshold have a higher variability. At high confluency, the variability of threshold values is very high. Median intensity value shows the lowest variability at any confluency level.

TABLE I. MEAN THRESHOLD VALUES FOR SCALED FLUORESCENCE INTENSITY (16 BIT INTEGER) AND THEIR RELATIVE VARIABILITY

Threshold	Confidence	Scaled intensity (Variability)		
		L	***M***	***H***
lower	5%	330 (28%)	270 (19%)	240 (84%)
median	50%	460 (31%)	390 (12%)	510 (71%)
upper	95%	780 (64%)	520 (14%)	940 (93%)

Level of confluency; low (L); medium (M); high (H). (Samples 1, 2, 3).

B. Reproducibility of assessment

Independent operators performed and repeated confluency reference visual assessment. Confluency reproducibility was calculated for visual assessment. The results for images at low (L) medium (M) and high (H) confluency (Samples 1) are showed in Table II. The calculation of confluency by visual assessment on images is reproducible at around 10% (L1), 5% (M1) and 3% (H1) relative reproducibility. The calculation method by mean area (double threshold) showed worse reproducibility at all confluency levels. The calculation method by median threshold (single threshold) showed the best reproducibility at all confluency levels.

TABLE II. CONFLUENCY MEAN VALUES (C) AND ITS EXPANDED REPRODUCIBILITY (U_R K=2) FOR A SINGLE IMAGE AT THE BEST FOCUS

Calculation method	*L1*		*M1*		*H1*	
	C	**U_R**	**C**	**U_R**	**C**	**U_R**
Visual	10.4%	0.9%	32.3%	1.5%	87.5%	3.0%
Mean Area	10.8%	1.5%	37.6%	2.3%	86.7%	7.2%
Mean Threshold	8.5%	0.7%	28.7%	1.4%	85.2%	6.8%
Median Threshold	9.3%	0.9%	29.4%	1.1%	88.2%	1.0%

Level of confluency; low (L); medium (M); high (H). (Samples 1).

C. Uncertainty of realization of confluency definition

The visual assessment estimation is here considered as a reference value. The four calculation methods are different ways to realize the definition of the confluency and are a source of uncertainty [32]. Uncertainty of calculation was evaluated for each visual assessment, Mean, min and max expanded contribution to uncertainty (k=2) of the way to define

the most probable free edge and its relevance compared to total calculated uncertainty are reported in Table III. The different ways to calculate confluency produce a relevant spread of values. The relevance of the contribution is lower than 20%, on the whole range of confluency (same order of magnitude of the total uncertainty) and gives a relevant contribution to total uncertainty (I_S>10%). The uncertainty and its variability are higher for medium confluency where the length of free edge is larger.

TABLE III. REALIZATION OF THE DEFINITION OF CONFLUENCY. UNCERTAINTY (U_M) AND SIGNIFICANT INDEX (I_S) OF ITS CONTRIBUTION TO TOTAL UNCERTAINTY

	L	M	H
U_M mean (k=2)	1.0%	6.2%	1.9%
U_M min (k=2)	0.3%	3.7%	0.2%
U_M max (k=2)	1.7%	10.7%	5.0%
I_S max	18%	19%	17%

Level of confluency; low (L); medium (M); high (H). (Samples 1,2,3).

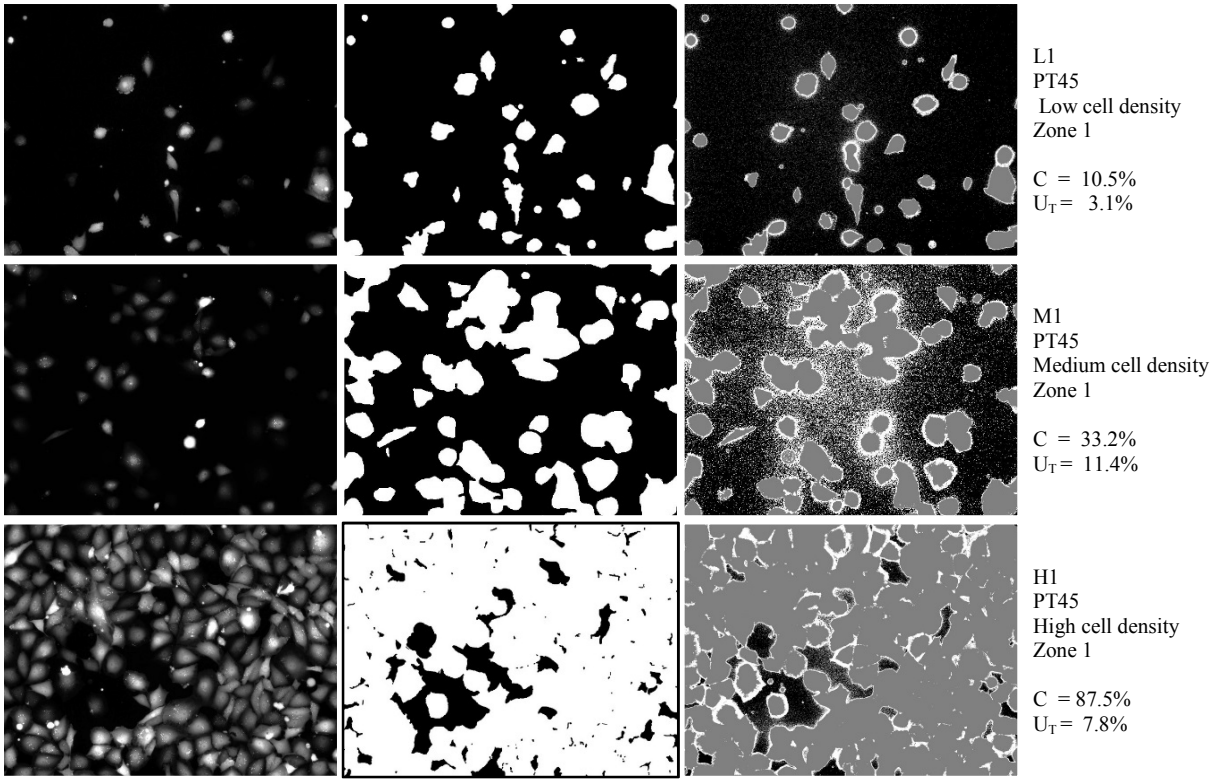

Fig. 3. Samples at low (L) medium (M) and high (H) level of confluency (Samples 1). Images of cells acquired with the camera; maps of the visual evaluation of surface covered by cells (white); three classes images: Background (black) Foreground (gray) and Boundary (white) with the algorithm implemented.

D. Uncertainty of a single threshold

The attribution of pixels with scaled intensity in between the lower and upper thresholds to background or foreground was considered uncertain for a single threshold confluency calculation. Absolute and relative expanded uncertainty (k=2 to give the 95% coverage of the range) are reported in Table IV for the nine samples. Expanded uncertainty resulted to be higher than the typical step in visual assessment of confluency, i.e., 5-10% for medium confluence. Relative expanded uncertainty resulted to be between 15% and 30% at low confluency, higher than 35% at medium confluency and lower than 10% at high confluency.

Figure 3 shows the visual representation of the results for low medium and high confluency (Sample 1). The scaled images acquired with the microscope camera, the map of the visual identification of cell surface and the three zone images (background black; foreground gray; boundary white) are reported for each sample.

TABLE IV. UNCERTAINTY (U_T) AND RELATIVE UNCERTAINTY (U_T/C) OF CONFLUENCY (C) FOR PIXEL ATTIBUTION BY A SINGLE THRESHOLD

Sample	U_T (U_T/C) (k=2)		
	L	*M*	*H*
1	3.1% (30%)	11.4% (35%)	7.8% (9%)
2	3.0% (27%)	24.5% (53%)	5.1% (5%)
3	1.2% (14%)	21.4% (53%)	5.8% (6%)

Level of confluency; low (L); medium (M); high (H). (Samples 1,2,3).

E. Focal planes effects

The effects of focal plane position on confluency and single threshold uncertainty were investigated. Confluency at best focus and its expanded variability due to the variation of focus plane are reported in Table V for low medium and high confluency (Samples 1). The significant index of variability is lower than 2% on the whole range of

confluency, it means that variability is not relevant (I_S<10%) and not negligible (I_S>1%).

TABLE V. 20 µM FOCUS PLANE VARIATION. BEST FOCUS VISUAL ASSESSMENT CONFLUENCY, ITS EXPANDED VARIABILITY (U_F), ITS RELATIVE VARIABILITY (U_F/C) AND SIGNIFICANCE INDEX (I_S) OF VARIABILITY CONTRIBUTION TO TOTAL UNCERTAINTY

	L1	M1	H1
C (Best focus)	10.4%	32.3%	87.5%
U_F (U_F/C) (k=2)	0.3% (3%)	1.6% (5%)	1.0% (1%)
I_S	1%	2%	2%

Level of confluency; low (L); medium (M); high (H). (Samples 1).

The uncertainty of attribution for a single threshold method was calculated for the three confluency levels from the images taken at different focal plane in zone 1 of each dish (Samples 1). Results are reported in Table VI. The variability of uncertainty is not relevant (I_S<10%) on the whole range of confluency.

TABLE VI. FOCUS PLANE VARIATION. SINGLE THRESHOLD UNCERTAINTY (U_T), ITS EXPANDED VARIABILITY (dU_T) AND SIGNIFICANCE INDEX (I_S) OF VARIABILITY CONTRIBUTION TO THRESHOLD UNCERTAINTY

Focal plane	L1	M1	H1
-10µm	2.7%	12.5%	6.3%
-5µm	2.9%	10.4%	6.7%
Best focus	3.2%	12.0%	6.8%
+5µm	3.0%	9.1%	7.1%
+10µm	2.8%	12.7%	6.6%
dU_T (k=2)	0.3%	2.1%	0.4%
I_S	1%	4%	1%

Level of confluency; low (L); medium (M); high (H). (Samples 1).

IV. DISCUSSION

The proposed algorithm calculate the uncertainty due to a single intensity level taken as threshold limit associated to a visual assessment, taken as a reference method. The reproducibility of visual assessment, the variability of the realization of confluency definition (corresponding to the most probable free edge between foreground and background), the variation of focal plane during image acquisition were considered as sources of uncertainty. The typical step of a traditional visual assessment (5-10%) can be considered as a reference value for actual uncertainty. The reproducibility of visual assessment was lower than the typical step. The uncertain attribution of pixels at the most probable scaled intensity (single threshold) gave the most relevant contribution to the total uncertainty for all images and visual assessments. The calculation method gave limited contribution to the total uncertainty for the most of assessments it gave a relevant contribution. The focal plane variation gave a not relevant contribution for both confluency value and single threshold uncertainty over the whole range of confluency. The uncertainty at medium level of confluency resulted to be higher of the typical step of a traditional visual assessment, while at low and high levels it resulted to be lower but close. Bias for threshold identification is not considered in this approach. The identification of the threshold value is often based on analyses of pixel intensity distribution that is performant when edges are well defined; the risk of biases is very high in the context here considered.

V. CONCLUSION

The typical approach of confluency calculation algorithms is the identification of an intensity threshold value that separate background from foreground, the proposed algorithm provides an upper and lower limit associated to a visual assessment, taken as a reference method. The algorithm calculate the uncertainty due to a single intensity level taken as threshold. It proposes a solution to the problem of assigning an estimate uncertainty to an analysis of confluency, to enhance reliability of measured values. The algorithm for the uncertainty estimation was tested on the whole range of confluency; it provided values in any conditions, i.e., it was efficient, values were correct, i.e., it was robust. The probability to have a correct estimation of the confluency uncertainty due to a single correct threshold value is high, i.e., the algorithm is reliable.

Routine biological analysis can easily embed the approach to compare visual assessment and automatic algorithms. The method has currently a part of visual assessment that requires the intervention of an operator. The automation of this part would allow the use of this algorithm for automatic analysis of HSC. The identification of free edges and multilevel approaches to confluency measurement could be much more effective than threshold approach, reducing pixel attribution uncertainty and the risk of biases. The representation of uncertainty as a numerical value and as the image of free edge of cells can simplify the understanding in multidisciplinary approaches where knowledge from different backgrounds are mixed in one team.

REFERENCES

[1] M. Götte , G. Hofmann , A. Michou-Gallani , J. F. Glickman, W. Wishart and D. J. Gabriel , "An imaging assay to analyze primary neurons for cellular neurotoxicity" Neurosci Methods, vol.192, pp.7-16, 2010.

[2] A. Xia and S. T. Wrong, "Concise review: a high-content screening approach to stem cell research and drug discovery" Stem cells, vol.30, pp.1800-1807, 2012.

[3] J.Alonso-Padilla, I. Cotillo, J. Cantizani and J. Presa, "Automated High-Content Assay for Compounds Selectively Toxic to Trypanosoma cruzi in a Myoblastic Cell Line" PLoS Negl Trop Dis, vol. 9, 2015

[4] D. Taylor, "Past, present, and future of high content screening and the field of cellomics" Methods Mol Biol, vol.356, pp.3-18, 2007.

[5] M. T. Bickle, "The beautiful cell: high-content screening in drug discovery" Anal Bioanal Chem, 398, 219-26, 2010

[6] A. H. Gough and P. A. Johnston, "Requirements, features and performance of high content screening platforms" Methods Mol Biol., vol.56, pp.1-61, 2007.

[7] R. Gonzalez, L. L. Jennings and M. Knuth, "Screening the mammalian extracellular proteome for regulators of embryonic human stem cell pluripotency" Proc Natl Acad Sci USA, vol.107, pp.3552–3557, 2010.

[8] B. R. Gorman, J. Lu, N. C. Lowry, J. E. Purvis and A. Baccei et al., "Multi-Scale Imaging and Informatics Pipeline for In

Situ Pluripotent Stem Cell Analysis" PLoS ONE, vol.9, pp.3116037, 2014.
[9] V. Ljosa and A. E. Carpenter , "Introduction to the Quantitative Analysis of Two-Dimensional Fluorescence Microscopy Images for Cell-Based Screening" PLoS Comput Biol, vol.5, e1000603, 2009.
[10] M. Ascenzi, X. Du, J. I. Harding, E. N. Beylerian, B. M. de Silva, B. J. Gross, H. K. Kastein, W. Wang, K. M. Lyons and H. Schaeffer, "Automated cell detection and morphometry on growth plate images of mouse bone Appl Math (Irvine), vol.5, pp.2866-2880, 2014.
[11] M. E. Berginski, S. J. Creed, S. Cochran, D. W. Roadcap, J. E. Bear and S. M. Gomez, "Automated analysis of invadopodia dynamics in live cells" PeerJ, vol.2, e462, 2014.
[12] C. Bühnemann, S. Li, H. Yu, H. Branford White, K. L. Schäfer, A. Llombart-Bosch, I. Machado, P. Picci, P. C. W. Hogendoorn, N. A. Athanasou, J. A. Noble, and A. B. Hassan, "Quantification of the Heterogeneity of Prognostic Cellular Biomarkers in Ewing Sarcoma Using Automated Image and Random Survival Forest Analysis" PLoS ONE, vol.9, e107105, 2014.
[13] L. Duan, T. Marvdashti, A. Lee, J. Y. Tang and A. K. Ellerbee, "Automated identification of basal cell carcinoma by polarization-sensitive optical coherence tomografy" Biomedical Optics Express, vol.5, pp.3717-3729, 2014.
[14] E. Sheik-Khalil, M. A. Bray, S. Ozkaya, G. Scarlatti, M. Jansson, A. E. Carpenter, E. M. Fenyo, "Automated image-based assay for evaluation of HIV neutralization and cell-to-cell usion inhibition" BMC Infectious Diseases, vol.14, pp.472, 2014.
[15] M. E. Digan, C. Pou, H. Niu and J. Zhang, "Evaluation of Division-Arrested Cells for Cell-Based High-Throughput Screening and Profiling", Journal of Biomolecular Screening, vol.10, 2005.
[16] Baradez M-O and D. Marshall, "The Use of Multidimensional Image-Based Analysis to Accurately Monitor Cell Growth in 3D Bioreactor Culture" PLoS ONE, vol.6, e26104, 2011.
[17] N. Jaccard, R. J. Macown, A. Super, L. D. Griffin, F. S. Veraitch, and N. Szita, "Automated and Online Characterization of Adherent Cell Culture Growth in a Microfabricated Bioreactor" Journal of Laboratory Automation, vol.19, pp.437-443, 2014.
[18] D. F. E. Ker, L. E. Weiss, S. N. Junkers, M. Chen, Z. Yin, M. F. Sandbothe, S.-il Huh, S. Eom, R. Bise, E. Osuna-Highley, T. Kanade and P. G. Campbell, "An Engineered Approach to Stem Cell Culture: Automating the Decision Process for Real-Time" PLoS ONE, vol.6, e27672, 2011.
[19] T. Y. Nguyen, C. G. Liew, and H. Liu., "An In VitroMechanism Study on the Proliferation and Pluripotency of Human Embryonic Stems Cells in Response to Magnesium Degradation" PLoS ONE, vol.8, e76547, 2013.
[20] S. Ahmadian, J. Barar, A.A. Saei, M.A.A. Fakhree, and Y. Omidi, "Cellular Toxicity of Nanogenomedicine in MCF-7 Cell Line: MTT assay" JoVE, vol.26, 2009.
[21] K. R. Jaiswal, H.-W. Xin, A. Anderson, G. Wiegand, B. Kim, T. Miller, D. Hari, S. Ray, T. Koizumi, U. Rudloff, S. S. Thorgeirsson, and I. Avital, "Comparative Testing of Various Pancreatic Cancer Stem Cells Results in a Novel Class of Pancreatic-Cancer–Initiating Cells" Stem Cell Res., vol.9, pp.249-260, 2012.
[22] F.J. Al-Saeedi, P.M. Mathew and V.A. Luqmani, "Assessment of Tracer 99mTc(V)-DMSA Uptake as a Measure of Tumor Cell Proliferation In Vitro" PLoS ONE, vol.8, e54361, 2013.
[23] P. Anderson, A. B. Carrillo-Galvez, A. Garcia-Perez, M. Cobo, and F. Martin, "(Endoglin)-Negative Murine Mesenchymal Stromal CellDefine a New Multipotent Subpopulation with Distinct Differentiation and Immunomodulatory Capacities" PLoS ONE, vol.8, e76979, 2013.
[24] Y.M. Efremov, A.A. Dokrunova, D.V. Bagrov, K.S. Kudryashova, O.S. Sokolova and K.V. Shaitan, "The effect of confluency on cell mechanical properties" Journal of Biomechanics, vol.46, pp.1081-1087, 2013.
[25] S.S. Hur, J.C. del Álamo, J.S. Park, YS Li, H.A. Nguyen, D. Teng, K.C. Wang, L. Flores, B. Alonso-Latorre, J.C. Lasheras and S. Chien, "Roles of cell confluency and fluid shear in 3-dimensional intracellular forces in endothelial cells" PNAS, vol.109, pp.11110-11115, 2012.
[26] O. Hayes, B. Ramos, L.L. Rodríguez, A. Aguilar, T. Badía and F.O. Castro, "Cell confluency is as efficient as serum starvation for inducing arrest in the G0/G1 phase of the cell cycle in granulosa and fibroblast cells of cattle," Animal Reproduction Science, vol.87, pp.181-192, 2005.
[27] S. Ghosh, H. Yanfen and L. Rong, "Cell Density is a Critical Determinant of Aromatase Expression in Adipose Stromal Cells" J Steroid Biochem Mol Biol, vol.118, pp.231-236, 2010
[28] M. Cho, T. Cho, J. M. Lim and J. Cho, "The establishment of mouse embryonic stem cell cultures on 96-well plates for high-throughput screening," Mol.Cells, pp.456-461, 2013.
[29] E. C. Metz, "Receiver operating characteristic analysis: a tool for the quantitative evaluation of observer performance and imaging systems" Journal of the American College of Radiology, vol.3, n.6, 2006.
[30] KW Eliceiri, MR Berthold, IG Goldberg, L Ibáñez, BS Manjunath, ME Martone, RF Murphy, H Peng, AL Plant, B Roysam, N Stuurman, N Stuurmann, JR Swedlow, P Tomancak, AE Carpenter, "Biological imaging software tools" Nat Methods, vol.9, pp.697-710, 2012.
[31] A.F. Hoffman and R. J. Garippa, "A pharmaceutical company user's perspective on the potential of high content screening in drug discovery" Methods Mol Biol, vol.356, pp.19-31, 2006
[32] JCGM100:2008, "Guide to the Expression of Uncertainty in Measurement JCGM100:2008 – GUM 1995 with minor corrections.," ISO, 2008.
[33] G. Sassi, A. Demichelis, M. Sassi, "Uncertainty analysis of the diffusion rate in the dynamic generation of VOC mixtures", Measurement Sci.Technol., vol.22, pp.105104, 2011.